ISSN: 0976-3031

Available Online at http://www.recentscientific.com

CODEN: IJRSFP (USA)

International Journal of Recent Scientific Research
Vol. 9, Issue, 12(C), pp. 29963-29969, December, 2018

International Journal of Recent Scientific Research

DOI: 10.24327/IJRSR

Research Article

STRUCTURAL AND OPTICAL STUDIES OF ZINC OXIDE NANORODS PREPARED BY HYDROTHERMAL TECHNIQUE

Jainulabdeen S[1]., Gopinathan C[1]*., Mumtaz Parveen A[2] and Saravanakumar K[3]

[1]School of Energy, Environment and Natural Resources Department of Solar Energy, Madurai Kamaraj University, Madurai-625021, Tamilnadu, India
[2]Faculty of Science, Orison Academy CBSE School, Coimbatore-641021, Tamilnadu, India
[3]Department of Physics, Kongunadu Arts and Science College, Coimbatore-641029, Tamilnadu, India

DOI: http://dx.doi.org/10.24327/ijrsr.2018.0912.2969

ARTICLE INFO

Article History:
Received 10th September, 2018
Received in revised form 2nd October, 2018
Accepted 26th November, 2018
Published online 28th December, 2018

Key Words:
ZnO Nanorod, growth mechanism, GIXRD, UV, FESEM and Raman.

ABSTRACT

The ZnO nanorods were fabricated by hydrothermally on induced seed layers by various concentrations of equi-molar of Zinc Nitrate Hexahydrate ($Zn(NO_3)_2.6H_2O$) and hexamethylenetetramine (HMTA). The crystal structure, orientation and optical properties were investigated by GIXRD and UV. Crystallite sizes and c/a ratio were calculated from Grazing Incidence X-ray diffraction (GIXRD) patterns whose values are decreased with increasing concentration. Optical properties were studied using UV – Visible Spectroscopy and strong absorption peaks observed at the wave length 379.5nm for higher concentration. The Raman studies are showed every E_2 (high) mode peak shifted to lower Raman frequencies compared with ZnO single crystal. FESEM image results are seen, the prepared ZnO nanorod structure have best crystalline nature of the material and all the films exhibited tensile stress, which can also confirmed by GIXRD results.

INTRODUCTION

Zinc oxide is widely used in different areas because of its unique electrical, optical, electronic, photocatalytic, dermatological and antibacterial properties [1-10]. For these applications, the nano-particles need to be dispersed homogeneously in the different matrices, and a number of new synthetic strategies have been developed in order to prevent particle agglomeration and increase the stability of zno nano particles dispersions. One dimensional (1D) ZnO nanostructure has following main advantages like, it is semi conductor, with direct bandgap of 3.37 eV, and a large excitation binding energy (60 meV) and higher melting point 1975^0C [3]. It is an important functional oxide, exhibiting excellent photo catalytic activity. Since of its noncentral symmetry, ZnO exhibits piezoelectric which is a property in building electrochemical coupled sensors and transducers [5]. And also ZnO is useful for the bio-safe and biocompatible in the field of biomedical applications [9]. From the said characteristics ZnO is only one of the nano material in future for current research and applications.

The preparation of ZnO thin films has been the subject of continuous research for a long time because the properties of ZnO films depends upon the method of preparation and practical application of ZnO can be modulated by varying its morphology [11-13]. Many number of reports are published ZnO structures such as nano wires, nanobelts, nanorods, nanotubes, nanoflowers [14-23].

Many researchers have studied the growth mechanism and modelled the hydrothermal growth of 1D ZnO structure [24-28]. In the present paper we revealed the growth mechanism of ZnO rod. The growth mechanism is systematically and elaborately studied at various precursor concentrations at constant deposition time. The structural investigation on the rod itself made with GIXRD and Raman spectroscopy.

Experimental Work

The ZnO nanorods were deposited on Quartz substrate by two step process such as preparation of seed layer by RF magnetron sputtering and growth of ZnO nanorods by hydrothermal technique. Before deposition, the quartz substrates were cleaned with chromic acid, ultrasonic bath, distilled water and

Corresponding author:* **Gopinathan C
School of Energy, Environment and Natural Resources Department of Solar Energy, Madurai Kamaraj University, Madurai – 625021, Tamilnadu, India

acetone processed by the following cleaning procedure to remove the unwanted impurities normally present on the surface of the quartz substrates when exposed to the atmosphere.

From the beginning seed layer is prepared by RF Magnetron Sputtering Unit. The sputtering procedure is commenced by evacuating the chamber to $1x10^{-6}$ mbar. The substrate temperature is fixed as 400°C using temperature controller. Ar (99.999%), being a noble gas which does not react with either the target or the substrate, is then introduced into the chamber at a specified pressure. The r.f. supply is then switched on and stabilized to the 200W power. The substrate to target distance is fixed as 5.5 cm. The deposition last for 8 min and the thickness obtained as 60 nm measured through quartz crystal thickness monitor.

After the preparation of ZnO seed layer, ZnO nanorods are grown on the seed layer by hydrothermal technique. In the preparation of ZnO nanorods, Zinc Nitrate Hexahydrate ($Zn(NO_3)_2.6H_2O$) and hexamethylenetetramine (HMTA) were used as source compounds which are dissolved in de-ionized water and the precursor solutions prepared with various equimolar concentrations of Zinc Nitrate and HMTA such as 0.05M, 0.075M, 0.15M and 0.2M on constant stirring at room temperature for 30 min. After continuous stirring the milky white solution was obtained. Then prepared seed layer was vertically immersed into the prepared solutions by placing seed layer facing against wall of the beaker. The beaker with the reactive solution was immersed into pre-heated water bath. The deposition was carried at constant time at 2 hours. The resulting films were homogeneous, well adhered to the substrate with light white color. After deposition, the substrates were rinsed in de-ionized water and dried at room temperature for overnight.

Preparation of Seed Layer

The quartz substrate is deposited by ZnO nanorods by two step process such as preparation of seed layer by RF magnetron sputtering and growth of ZnO nanorods by hydrothermal technique. prior to deposition, the quartz substrates were cleaned with chromic acid, ultrasonic bath, distilled water and acetone processed by the following cleaning procedure to remove the unwanted impurities normally present on the surface of the quartz substrates when exposed to the atmosphere.

Initially seed layer is fabricated by RF Magnetron Sputtering Unit. The sputtering procedure is commenced by evacuating the chamber to $1x10^{-6}$ mbar. The substrate temperature is fixed as 400°C using temperature controller. Ar (99.999%), being a noble gas which does not react with either the target or the substrate, is then introduced into the chamber at a specified pressure. The r.f. supply is then switched on and stabilized to the 200W power. The substrate to target distance is fixed as 5.5 cm. The deposition last for 8 min and the thickness obtained as 60 nm measured through quartz crystal thickness monitor.

Formation of ZnO Nanorods

After the preparation of ZnO seed layer, ZnO nanorods are grown on the seed layer by hydrothermal technique. In the preparation of ZnO nanorods, Zinc Nitrate Hexahydrate ($Zn(NO_3)_2.6H_2O$) and hexamethylenetetramine (HMTA) were used as source compounds which are dissolved in de-ionized water and the precursor solutions prepared with various equimolar concentrations of Zinc Nitrate and HMTA such as 0.05M, 0.075M, 0.15M and 0.2M on constant stirring at room temperature for 30 min. After continuous stirring the milky white solution was obtained. Then prepared seed layer was vertically immersed into the prepared solutions by placing seed layer facing against wall of the beaker. The beaker with the reactive solution was immersed into pre-heated water bath. The deposition was carried at constant time at 2 hours. The resulting films were homogeneous, well adhered to the substrate with light white color. After deposition, the substrates were rinsed in de-ionized water and dried at room temperature for overnight.

Characterization tools used

The structural properties of ZnO nanorods on seeded layer are measured in Bruker D8 advance GIXRD using CuKα radiation and Raman studies are carried out by Raman spectrometer of Horiba Model: Xplora Plus. FESEM evidenced that grown film as a rod structure ZnO. Both the crystalline and optical studies are well explained about ZnO is grown as a rod structure.

RESULTS AND DISCUSSION

Structural Studies

The GIXRD patterns of ZnO nano structured thin films grown in equimolar concentrations of Zinc Nitrate and HMTA such as 0.05M, 0.075M, 0.15M and 0.2M equi-molar of Zinc Nitrate Hexahydrate ($Zn(NO_3)_2.6H_2O$) and hexamethylenetetramine (HMTA) is shown in Fig. 1.

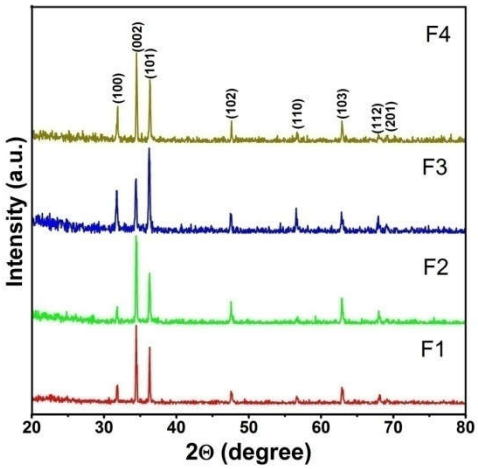

Fig 1 GIXRD pattern of ZnO nanorods

It can be seen from GIXRD data, that all the samples are polycrystalline in nature and the crystallites are preferentially oriented along (002) plane of c axis [29]. The datas are well matched with the JCPDS card no.01-070-255 which exhibit single phase ZnO hexagonal wurtzite structure with no other secondary phase. c axis (002) oriented [29] and matched with the JCPDS card no.01-070-255. In addition to the (002) peak, other peaks such as (100), (101), (102), (110), (103), (112) and (201) are observed. The '*C*' axis orientation may be a common phenomenon in ZnO film deposition by chemical process using organo-zinc compounds. In hexagonal wurtzite ZnO, the top and bottom of basal planes are corresponds to (0001) and $(000\bar{1})$ terminated with polar ions Zn^{2+} and O^{2-}. Hence the

positive and negative surfaces attracted the opposite ions and then the layers stacked alternatively and forms nanorods grow along c axis. Since the side facets $\{01\bar{1}0\}$ are non-polar in nature and due to less surface energy the growth along the side facets generally does not take place much [30].

From the peak position, the crystallite size of the nanorod structured films are calculated from the Debye-Scherrer formula [31],

$$D = 0.9\lambda/\beta Cos\Theta \quad (1)$$

Where D is the mean particle size, λ = 0.15406 nm is the x-ray wavelength, θ is the Bragg diffraction angle and β is the full width at half maximum (FWHM) of the diffraction peak, respectively. Then the lattice constants a, b and c values are calculated form the following relation [31],

$$\frac{1}{d^2} = \frac{4}{3}\left(\frac{h^2 + hk + k^2}{a^2}\right) + \frac{l^2}{c^2} \quad (2)$$

Where h,k,l are miller indices of respective plane and d is the interplanar distance. The values of crystallite size, lattice constants and c/a ratios are given in Table 1.

Table 1 Structural Parameters and optical parameters of ZnO Nanorods calculated from XRD and Bandgap calculated from PL.

Sample Code & Molarity	Crystallite Size D(nm)	Dislocation Density δ x10^{15} Lines/metre	Strain t x10^{-3}	Lattice parameter a	b	C	c/a ratio	Bandgap (eV)
F1& 0.05M	76.1417	0.2019	0.4803	3.2485	3.2485	5.2008	1.60099	3.1
F2&0.075M	57.4251	0.3607	0.6395	3.2481	3.2481	5.2044	1.60229	3.21
F3&0.15M	57.8489	0.4191	0.6812	3.2519	3.2519	5.2085	1.60168	3.32
F4&0.2M	42.8726	0.4780	0.8487	3.2539	3.2539	5.2098	1.60109	3.64

The lattice constant values are very closely matches with the JCPDS card no. number 01-070-2551 of a=b=3.2490A^0 and c = 5.2070A^0. The crystallite size is decreasing from 76.14nm to 42.87nm with increasing concentration from 0.05M to 0.2M. There is no much variations constant value found in c/a ratio with respect to varying concentration. It is observed from the peak positions that the orientation of growth of rod is varying with respect to various concentration. Since the GIXRD exhibits the diffraction pattern of approximately 100 nm layer thickness from the surface, this small variation in c/a ratio is purely due to the orientation effect.

Using above the following tangent formula [32], the lattice strain (ε_{av}) has been calculated.

$$\varepsilon_{av} = \beta / \tan\Theta \quad (3)$$

The dislocation density (δ), which represents the amount of defects in the crystal, is estimated from the following equation [33].

$$\delta = 1/D^2 \quad (4)$$

It is observed that both lattice strain and dislocation density is increased with increase of equimolar concentration of Zinc Nitrate and HMTA from 0.05M to 0.2M. Also it is noted that the crystallite size of ZnO is decreased from 76.14nm to 42.87nm. The reason for increasing crystal defects can be identified from the decrease in size of the crystallites. In the growth of nanorods, increasing the concentration thereby increases the Zn^{2+} and O^{2-} ions in the bath solution which promotes more nucleation sites on the substrate. During the growth, the formation of bigger crystals is hindered by the growth of individual crystallites from the nucleation sites and therefore the size of the growing crystallite is reduced. Here it is clearly observed and identified that the concentration of precursor is influencing the size of the crystals in the growth.

It can be observed that dislocation density decreases with increase of Zn concentration which showed that the Zn^{2+} concentration plays an important role in size.

Growth Mechanism

ZnO nanorod growth takes place on seeded substrate by hydrothermal method. The precursors used in the hydrothermal process are In hydrothermal growing process we used Zinc Nitrate Hexahydrate ($Zn(NO_3)_2.6H_2O$) and hexamethylenetetramine (HMTA) chemicals. The mechanism of ZnO rod growth is reported by several researchers [34, 35]. But all the reports are not exactly reveal the role of HMTA [36]. The chemical equations for the formation of ZnO rod in the hydrothermal method is as follows [34, 37],

$$HMT + 6H_2O \leftrightarrow 4NH_3 + 6HCHO \quad (5)$$

$$NH_3 + H_2O \leftrightarrow NH_4{}^+ + OH^- \quad (6)$$

$$Zn^{2+} + 4NH_3 \leftrightarrow [Zn(NH_3)_4]^{2+} \quad (7)$$

$$Zn^{2+} + 2OH^- \leftrightarrow Zn(OH)_2 \quad (8)$$

$$Zn(OH)_2 \leftrightarrow ZnO + H_2O \quad (9)$$

Fig.2. shows the 3D AFM images of ZnO nanorods. When the equimolar concentrations of Zinc Nitrate and HMTA concentration of the solutions increases from 0.05M to 0.2M, the rod started to grow preferentially on *C* axis along (002) direction and density of the rod also increased. The increase in number of rods and decrease in size of rods are observed while increasing the concentration. These results are well correlated with GIXRD results. This is due to the increase of vertical and lateral growth of rod which can also confirmed by GIXRD results.

The morphologies of fabricated ZnO nanorods are studied by FESEM images are shown in Fig.3. It can be seen clearly that the concentration is an important factor which has influence on the dimension of the nanorods. The concentration of these Zn^{2+} and O^{2-} ions exceeds a critical value, then ZnO nuclei starts. In Fig. 3a. Some of places of surface has more ZnO crystals and some places are empty. It is due to the ZnO nucleus is formed on the energetically favourable nucleation sites on the seed layer. After ZnO nuclei forms, Zn^{2+} and O^{2-} ions start to build up at this local position. Due to the crystal structure of ZnO building up is bigger in (0001) crystal plane direction than other crystal plane [37]. Also it is reported that (0001) direction has the fastest growth rate and $(000\bar{1})$ direction has the slowest growth rate [30]. The average diameter of ZnO nanorods fabricated in 0.05M, 0.075M, 0.15M and 0.2M equimolar

concentrations of zinc nitrate and HMTA aqueous solutions are 322 nm, 312nm, 333nm and 322nm respectively.

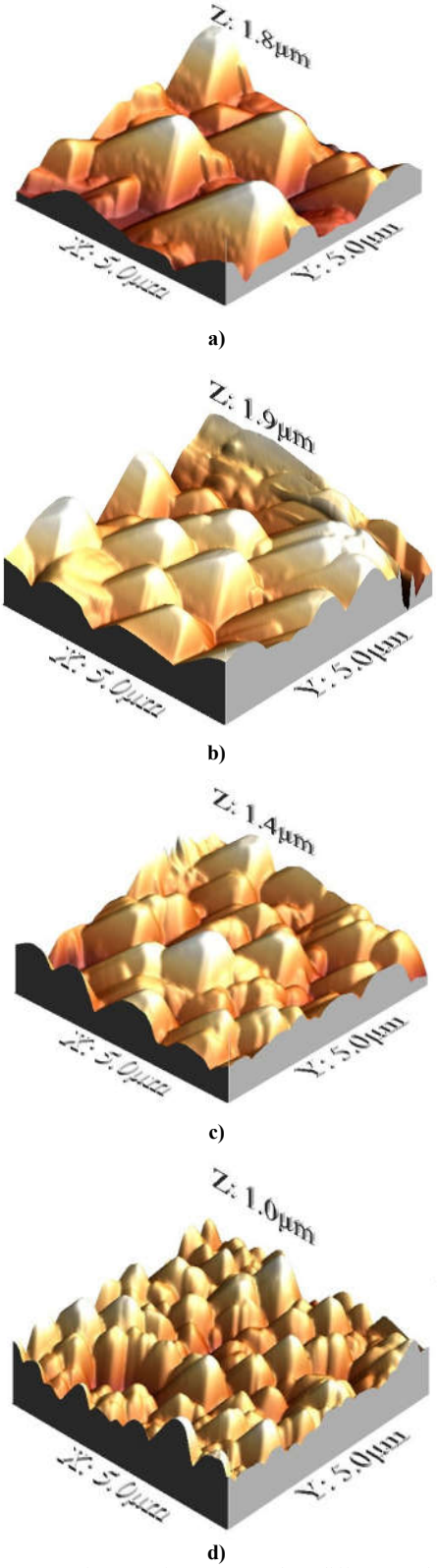

Fig 2 3D AFM images of ZnO nanorods at different equimolar concentrations of Zin Nitrate and HMTA conentration such as a) 0.05M, b) 0.075M, c) 0.15M and d) 0.2M

The density of nanorod increased with increase of concentrations and spreads over entire surface. Furthermore it is clearly observed from the FESEM images that when increasing the concentration, the orientation of rod on vertical axis increases and at 0.2M concentration, all the rods are vertically aligned perpendicular to surface. This vertical alignment of rods are very important in fabricating all devices especially luminescence and sensors. At this morphology, the transport of charge carriers in vertically aligned rods are quite high due to less annihilation. The hexagonal facets are clearly observed on the top of rod surface (Fig.3) and this clearly evidenced the structure of ZnO is hexagonal in nature and it is also found that the nanorods are uniformly aligned on the surface.

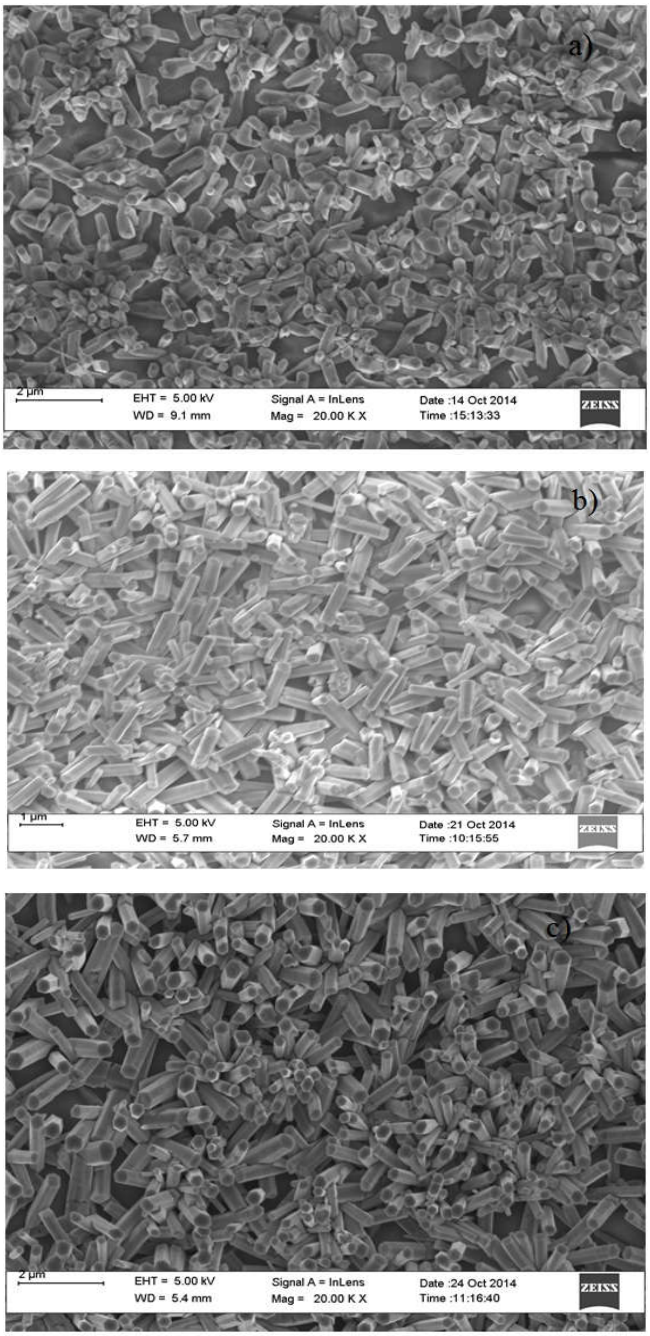

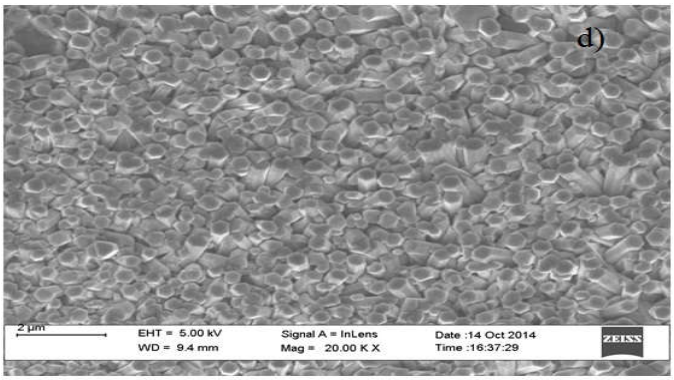

Fig 3 FESEM images of ZnO nano rods at different concentration a) 0.05M, b) 0.075M, c) 0.15M and d) 0.2M

Optical Properties

The Beer-Lambert law states that the absorbance of a solution is directly proportional to the solution's concentration. The absorbance graph of ZnO nanorod grown at various equimolar concentrations of Zinc Nitrate and HMTA for the constant reaction time 2 hours is shown in Fig. 4.

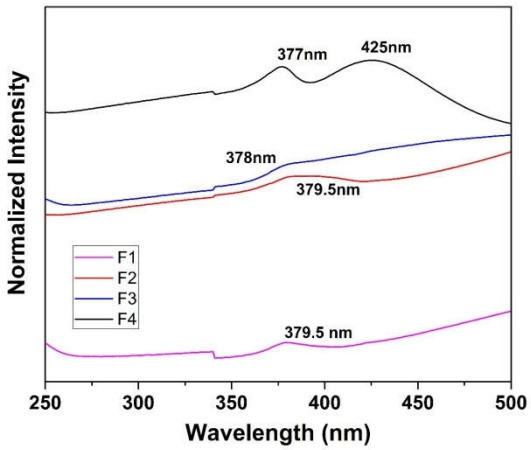

Fig 4 Absorbance graph of ZnO nanorod grown at various equimolar concentrations of Zinc Nitrate and HMTA

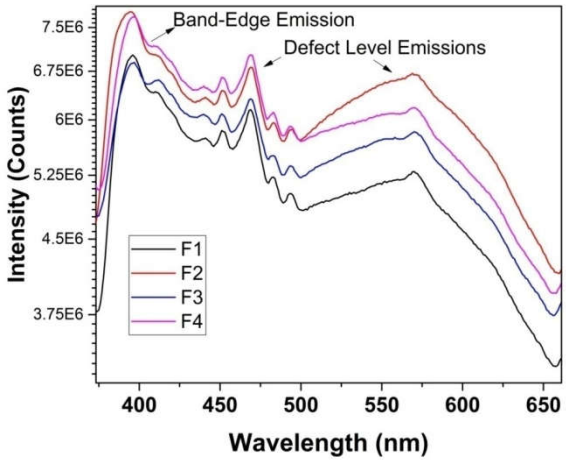

Fig 5 PL Spectrum of ZnO nanorod grown at various concentrations

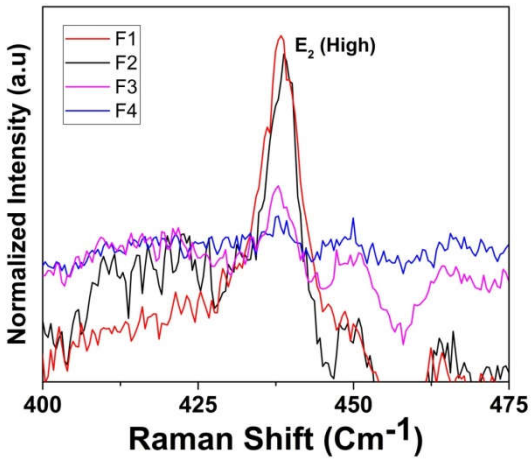

Fig 6 Raman Spectrum of ZnO nanorod grown at various concentrations

If the concentration increases from 0.05M to 0.2M, the strong absorption peak also increased and it is observed at 379.5nm. This absorption peak is blue red shifted and this as compared to the bulk exciton absorption of ZnO (373 nm) [39] which are due to the size effect of the nanostructures. At 0.2M concentration, the absorption in the visible range centered at 425nm is observed which implied more defect energy levels in the prepared ZnO nanostructures [41]. Band gap is calculated from the tauc plot from the absorbance spectrum and the same is given in Table 1. The bandgap energy values are red blue shifted from 3.64eV to 3.32eV when increasing concentration at constant time 2 hours. This is due to quantum confinement effect of charge carriers. the vertical and lateral growth of ZnO nano rod.

Since NBE emission is exactly originated from the band edges, the bandgap of the material must be exactly equal to the emission energy of NBE. The bandgap values are represented in Table 1.

PL spectrum of ZnO rod grown at different concentrations for the reaction time 2 hours is shown in Fig. 5. It is observed that ZnO samples exhibit strong UV emission around 3.32eV. The emission around 3.32 eV is originated by transitions of electron between the bottom of conduction band to the top of valence band and it is so called near band-edge emission (NBE). NBE comes from the recombination of free excitons at valence band, whereas the visible emission attributed to the deep level emission (DLE), originates from the exciton recombination in the localized states. The localized states is created may be due the deep donor defects such as Zinc interstitials (Zn_i), Zinc-Oxygen antisites (Zn_O) and Oxygen vacancy (V_O).

Raman spectra of the film were taken in order to confirm the presence of wurtzite phase and crystal quality in the ZnO rod. ZnO in the hexagonal structures with C_{6V}^4 symmetry each unit cell has 4 atoms and occupies 2b site of symmetry. The group theory predicts, the wurtzite ZnO has eight set of characteristic optical phonon modes at the centre of Brillouin zone (r point)

$$r = 1A_1+2B_1+1E_1+2E_2 \quad (10)$$

From above equation both A_1 and E_1 modes are polar and split into transverse (TO) and longitudinal optical (LO) phonons with different frequencies. Two non polar E_2 and B_1 modes are Raman active and silent mode. The raman spectrum of ZnO nanorod grown at various equimolar concentrations of Zinc

Nitrate and HMTA is shown in the figure 6. It is noted that only strong peak around 438Cm^{-1} is observed in the spectrum and other peaks are could not be visible due to higher value of signal to noise ratio. The E_2(High) raman active mode of ZnO, relates the characteristic wurtzite phase of ZnO rods, orientation along c axis and crystalline quality. Here in both the concentrations, the peak intensity of E_2(high) is predominant over the other peaks indicates that the obtained ZnO nanorods are in hexagonal wurtzite phase with high crystalline quality. It is observed that while increasing the equimolar concentration the intensity of peak is increases indicates that nanorods are crystallised in hexagonal wurtzite phase with higher crystalline quality and improved in the orientation of nanorods in c axis at higher concentration.

If a tensile stress occurs in the sample, The E_2(high) peak can shift to lower frequencies compared with bulk value of 438 cm^{-1}, while the E_2(high) peak can shift to higher frequencies compared with bulk value of 438 cm^{-1}, if there exists a compressive stress in the ZnO rod.

It can be seen from Fig.6, the position of each E_2(high) peak also shifted to lower frequencies compared with ZnO bulk crystal [40]. From this result, the prepared ZnO rods have the best crystal quality and all the films exhibited tensile stress, which can also confirmed by GIXRD results.

CONCLUSION

The ZnO nanorods were fabricated by hydrothermally on induced seed layers by various concentrations of equi-molar of Zinc Nitrate Hexahydrate ($Zn(NO_3)_2.6H_2O$) and hexamethylenetetramine (HMTA). The crystal structure, orientation and optical properties were investigated by GIXRD and UV. Growth mechanism of C-axis oriented ZnO nanorods has been studied with XRD, FESEM and AFM. Optical properties revealed that ZnO nano rods having absorption at UV region of 377 nm which have increased of precursor concentration. Photo-luminescence spectrum exhibits the UV light emission and the same in increasing with increasing precursor concentration.

References

1. Si Nae Heo, Keun Young Park, Young Jun Seo, Faheem Ahmed, M. S. Anwar, and Bon Heun Koo, Electron Mater. Lett. Vol. 9 (2013) 261-265.
2. P. Zu, Z.K. Tang, G.K.L. Wong, M. Kawasaki, A. Ohtomo, H. Koinuma and Y. Segawa, Solid State Communications 103 (1997) 459.
3. A. Sakthivelu, V. Saravanan, M. Anusuya, J. Joseph Prince, *Journal of Ovanic Research*, 7 (2011) 1-7.
4. S. Lopez-Romero, M. Garcia-H, World *Journal of Condensed Matter Physics*, 3 (2013) 152- 157.
5. C. Amutha, A. Dhanalakshmi, B. Lawerence, K. Kulathuraan, V. Ramadas, B. Natarajan, Progress in Nanotechnology and Nanomaterials, 3 (2014) 13-18.
6. NANDA SHAKTI, SUNITA KUMARI, P.S.GUPTA, Journal of Ovanic Research, 7 (2011) 51-59.
7. Slimane Haffad, Giancarlo Cicero, Madani Samah, Energy Procedia 10 (2011) 128-137.
8. Sankara Reddy B., Venkatramana Reddy S., Koteeswara Reddy N., Pramoda Kumari J., *Res. J. Material Sci*. 1 (2013) 11-20.
9. G. Poongodi, R. Mohan Kumar, R. Jayavel, *Int. J. ChemTech Res*. 6 (2014) 2026-2028.
10. Durata Haicu, Samim Saner, Onur Turdogru, Ugur Unal, Frontiers in Science 3 (2013) 96-101.
11. K. B. Lee, K. S. Cho, and H. Kwon, Met. Mater. Int. 15 (2009) 649.
12. J. S. Yi, J. Y. Kim, H. G. Jin, S. M. Song, C. H. Choi, W. T. Nicols, and W. I. Park, Met. Mater. Int. 18 (2012) 845.
13. W. I. Park, Met. Mater. Int. 14 (2008) 659.
14. Mohammad Reza Khanlary, Vahid Vahedi and Ali Reyhani, Molecules 17 (2012) 5021- 5029.
15. Hanmei HU, Xianhuai Huang, Chonghai Deng, Xiangying Chen, Yitai Qian, Materials Chemistry and Physics 106 (2007) 58-62.
16. Y. Xi, C. G. Hu, X. Y. Han, Y. F. Xiong, P. X. Gao, G. B. Liu, Solid State Communication 141 (2007) 506-509.
17. Chunfu Lin, Hong Lin, Jianbao Li, Xin Li, *Journal of Alloys and Compounds* 462 (2008) 175 -180.
18. Jian-jiao ZHANG, Er-jun GUO, Li-ping WANG, Hong-yan YUE, Guo-jian CAO, Liang SONG, Trans. Nonferrous Met. Soc. China 24 (2014) 736-742.
19. Ahmed H. Kurda, Yousif M. Hassan, Naser M. Ahmed, World *Journal of Nano Science and Engineering* 5 (2015) 34-40.
20. Bin Liu and Hua Chun Zeng, Nano Res 2 (2009) 201-209.
21. Yi Xi, Jinhui Song, Sheng Xu, Rusen Yang, Zhiyuan Gao, Chenguo Hu and Zhong Lin Wang, J. Mater. Chem. 19 (2009) 9260-9264.
22. GAO Hai-Yong, YAN Fa-Wang, ZHANG Yang, LI Jin-Min, ZENG Yi-Ping, Chin. Phys. Lett. 25 (2008) 640
23. Ye Yun,Guo Tailiang and Jiang Yadong, J. Semicond. 33 (2012) 4
24. Quanchang Li, Vageesh Kumar, Yan Li, Haitao Zhang, Tobin J. Marks, and Robert P. H. Chang, Chem. Mater. 17 (2005) 1001.
25. Shu-Yi Liu, Tao Chen, JingWan, Guo-Ping Ru, Bing-Zong Li, Xin-Ping Qu, ApplPhys A 94 (2009) 775.
26. D. Polsongkram, P. Chamninok, S. Pukird, L. Chow, O. Lupan, G. Chai, H. Khallaf, S. Park, A. Schulte, Physica B 403 (2008) 3713.
27. Francisco Solís-Pomar, Eduardo Martínez, Manuel F Meléndrez and Eduardo Pérez- Tijerina, Nanoscale Research Letters 6 (2011) 524.
28. VincenzinaStrano, Riccardo Giovanni Urso, Mario Scuderi, Kingsley O. Iwu, Francesca Simone, Enrico Ciliberto, CorradoSpinella and Salvo Mirabella, *J. Phys. Chem. C* 118 (2014) 28189.
29. Jian-jiao ZHANG, Er-jun GUO, Li-ping WANG, Hong-yan YUE, Guo-jian CAO, Liang SONG, Trans. Nonferrous Met. Soc. China 24 (2014) 736-742.
30. W.J. Li, E.W. Shi, W.Z. Zhong and Z.W. Yin, J. Cryst. Growth 203 (1999) 186.
31. B.D. Cullity, D.J. Cookson, R.F. Garrett, Elements of X-ray diffraction, 2nd ed.: Addison-Wesley: Reading, MA, 1978; p. 102.
32. K.Swaroop and H.M.Somashekarappa, *Research Journal of Recent Sciences* 4 (ISC-2014) 197-201.
33. C.Amutha, A.Dhanalakshmi, B.Lawrence, K.Kulathuraan, V.Ramadas, B.Natarajan Progress in Nanotechnology and Nanomaterials 3 (2014) 13-18.

34. D. Polsongkram, P. Chamninok, S. Pukird, L. Chow, O. Lupan, G. Chai, H. Khallaf, S. Park, A. Schulte, Physica B 403 (2008) 3713.
35. Sheng Xu and Zhong Lin Wang, Nano Research 4 (2011) 1013.
36. Conor P. Burke-Govey and Natalie O. V. Plank, *Journal of Vacuum Science & Technology* B 31 (2013) 06F101.
37. Q. Ahsanulhaq, A. Umar and Y. B. Hahn, Nanotechnology 18 (2007) 115603
38. W. Ostwald. Lehrbuch der AllgemeinenChemie, vol. 2, (1896) part 1. Leipzig, Germany.
39. M.Haase, H.Weller, A.Henglein, *J. Phys. Chem*., 92 (1988) 482.
40. N.Ashkenov, B.N.Mbenkum, C.Bundesmann, V.Riede, M.Lorenz, D.Spemann, E.M.Kaidashev, A.Kasic, M.Schubert, M.Grundmann, G.Wagner, H.Neumann, V.Darakchieva, H.Arwin and B.Monemar, *J. Appl. Phys.* 93 (2003) 126.

How to cite this article:

Jainulabdeen S *et al*.2018, Structural And Optical Studies of Zinc Oxide Nanorods Prepared By Hydrothermal Technique. *Int J Recent Sci Res.* 9(12), pp. 29963-29969. DOI: http://dx.doi.org/10.24327/ijrsr.2018.0912.2969

****